

# Resolution analyses for selecting an appropriate airborne electromagnetic (AEM) system

Niels B. Christensen<sup>1,3</sup> Ken C. Lawrie<sup>2</sup>

<sup>1</sup>Department of Geosciences, University of Aarhus, Aarhus, DK-8000 Aarhus C., Denmark.

<sup>2</sup>Geoscience Australia, GPO Box 378, Canberra, ACT 2601, Australia.

<sup>3</sup>Corresponding author. Email: nbc@geo.au.dk

**Abstract.** The choice of an appropriate airborne electromagnetic system for a given task should be based on a comparative analysis of candidate systems, consisting of both theoretical considerations and field studies including test lines.

It has become common practice to quantify the system resolution for a series of models relevant to the survey area by comparing the sum over the data of squares of noise-normalised derivatives. We compare this analysis method with a resolution analysis based on the posterior covariance matrix of an inversion formulation. Both of the above analyses depend critically on the noise models of the systems being compared. A reasonable estimate of data noise and other sources of error is therefore of primary importance. However, data processing and noise reduction procedures, as well as other system parameters important for the modelling, are commonly proprietary, and generally it is not possible to verify whether noise figures have been arrived at by reasonable means. Consequently, it is difficult – sometimes impossible – to know if a comparative analysis has a sound basis. Nevertheless, in the real world choices have to be made, a comparative system analysis is necessary and has to be approached in a pragmatic way involving a range of different aspects.

In this paper, we concentrate on the resolution analysis perspective and demonstrate that the inversion analysis must be preferred over the derivative analysis because it takes parameter coupling into account, and, furthermore, that the derivative analysis generally overestimates the resolution capability. Finally we show that impulse response data are to be preferred over step response data for near-surface resolution.

**Key words:** electromagnetic, resolution analysis, system comparison, time domain.

Received 13 January 2012, accepted 8 June 2012, published online 5 July 2012

## Introduction

Over the past decade, several new airborne electromagnetic (AEM) systems have seen the light of day, and when a new survey involving AEM is planned, one of the crucial choices is to select a proper system. A conscious and rational decision-making process is needed to reach a balanced decision that must necessarily be a compromise between many, often conflicting, interests and criteria. An important criterion is an analysis of the resolution capability of different AEM systems with regard to the models expected in the survey area and the aims of the investigation.

This paper is one of the results of a hydrogeophysical mapping project conducted by Geoscience Australia. Preliminary analyses concluded that an AEM survey combined with drilling would best help to achieve the aim of the survey. Among the systems considered were the TEMPEST, SkyTEM and the VTEM system, the first a fixed-wing system and the other two helicopterborne systems.

The main aspects of the selection process were:

- a phase 1 analysis of the resolution capability of different systems;
- a more thorough analysis of SkyTEM and TEMPEST, the two AEM systems that were shortlisted as realistic candidates from the first analysis;
- test lines flown with both systems;
- comparison of test line inversion results, both from contractor and in-house inversion;

- a comparison of inversion results with borehole induction logs;
- a set of practical criteria such as availability of systems, turnaround time for data, cost, etc.

A weighted assessment of the degree to which the above requirements could be satisfied by the two systems resulted in the SkyTEM system being chosen for the survey and subsequently a major survey was undertaken.

Ever since quantitative modelling and inversion methods became available to geophysicists for interpretation of field data, finding measures of the trustworthiness of the solution obtained has been a major concern. One way is to vary a model parameter and assess the difference between the model responses, often normalised by a measure of the data noise. This sensitivity measure was one of the first approaches to solution appraisal, but it is still used extensively. In the conceptual framework of inversion theory, the sensitivities are the derivatives of the model response with respect to model parameters. In situations where the number of model parameters is very large, or where model responses are computationally challenging, e.g. in 2D and 3D modelling and inversion, this approach can sometimes be the only feasible one.

Derivative analyses have been used extensively in connection with experimental design or the comparison of different EM methods. Examples illustrating this approach in Australia, where the methodology has officially been designated as best practice and the method of choice, are given

in Green and Munday (2004), Munday et al. (2003) and Fitzpatrick and Munday (2005). The methodology is used in Christiansen and Auken (2010) to derive a measure of the depth of investigation for electrical and electromagnetic methods. Recent applications (Brown et al., 2012) include the analysis of the effects of anisotropy in CSEM investigations.

Other measures are derived within the framework of inversion theory, such as the posterior model covariance matrix (MCM) that, given the data uncertainty, expresses the uncertainty of the inversion model parameters. The matrix contains the parameter variance and the covariance between model parameters. Inversion analysis using the MCM has been used frequently to assess the inversion model parameter uncertainty of different electromagnetic geophysical methods. Baumgartner and Christensen (1998) presented inversion of deep water geoelectrical soundings of the bottom sediments of Lake Geneva and an analysis of what the unconventional sounding method could achieve. The possibility of determining the coefficient of anisotropy in joint inversion of galvanic and electromagnetic data was investigated in Christensen (2000), and Christensen and Sørensen (2001) used the same methodology for experimental design studies of the pulled array geoelectrical sounding method (PACES). The potential of frequency domain helicopterborne (HEM) measurements to determine subsurface structure was analysed by Tølbøll and Christensen (2006) in connection with the development of an integrated strategy for inversion of HEM data, and for airborne TEM data by Christiansen and Christensen (2003). The potential of distinguishing resistive formations in one-dimensional (1D) inversion of CSEM data and its consequences for identifying the presence of oil and gas below the sea bottom was analysed in Christensen and Dodds (2007).

Another measure used in model appraisal is the model resolution matrix (MRM) that expresses the parameters of the estimated model as linear combination of the parameters of the 'true' model, and how each parameter of the true model contributes to the parameters of the estimated model (Menke, 1989). In the analyses of this paper, the MRM is identical to the unity matrix and therefore not very informative in relation to model appraisal.

Though we do not in a strict sense use the resolution measure of the MRM, we will in this paper use the word 'resolution' in the more broad sense of the word, indicating that a model feature can be inferred with a small posterior uncertainty.

More recent than the methods just mentioned are the Bayesian approaches, e.g. Markov chain Monte Carlo (MCMC) methods, that have gained practical importance with increasing computer speed and development of efficient sampling schemes of the model parameter space (e.g. Malinverno, 2002; Brodie and Sambridge, 2006; Gunning et al., 2010; Minsley, 2011). For each dataset, millions of models are tested with regard to fitting the data and statistical measures are found for the characteristics of the models fitting the data within the data uncertainty. The Achilles heel of the MCMC methods is that they still require considerable computer capacity, but they provide fully nonlinear statistics while inversion approaches most often linearise this analysis.

Yet another method of solution appraisal that lends itself also to 2D and 3D inversion problems is presented by Oldenburg and Li (1999). By initialising the inversion with a series of different models, the model features that remain constant are the ones that can be trusted while the ones that vary with the initial model are poorly resolved.

In this paper, we concentrate on the resolution analysis perspective and the issues involved in performing a

trustworthy analysis. We compare two different modes of performing an analysis of resolution capability: one based on the sum over all data of the squares of noise-normalised derivatives of the data with respect to the model parameters, in the following referred to as the derivative analysis; and one based on the estimates of parameter uncertainty derived from the posterior covariance matrix of a least-squares inversion formulation, in the following referred to as the inversion analysis. We argue that the latter is to be preferred as it takes coupling between the model parameters into account.

Using the inversion analysis, we compare the resolution capability of the SkyTEM and TEMPEST systems with regard to the model parameters of a series of five-layer models deemed representative for the survey area. We also compare the resolution capability of impulse and step response systems in general and show that impulse response systems have a better near-surface resolution, particularly in a conductive environment. Finally we compare inversion with multi-layer models of theoretical, noise-perturbed data from the five-layer models for the two systems. Throughout the paper, we attempt a discussion of the issues involved in providing the necessary information from the contractors to enable a reliable comparative analysis.

## Comparison of analysis methods and data types

### *Inversion analysis*

In the following sections, we compare the SkyTEM (Sørensen and Auken, 2004) and TEMPEST (Lane et al., 2000) AEM systems with regard to the uncertainty with which they will be able to determine the parameters, layer resistivities and thicknesses, in a one-dimensional (1D) model. The estimates of model parameter uncertainty are given by a linear approximation to the posterior model covariance matrix,  $C_{est}$ , given by

$$C_{est} = [G^T C_{obs}^{-1} G]^{-1} \quad (1)$$

where  $G$  is the Jacobian of the model (Inman et al., 1975) containing the derivatives of the response with regard to the logarithm of the model parameters:  $G_{ij} = \partial r_i / \partial \log p_j$  and  $C_{obs}$  is the data error covariance matrix. The noise on the data is assumed to be uncorrelated and log-normal distributed so that  $C_{obs}$  is a diagonal matrix containing the data variances. The *a posteriori* model parameter uncertainty estimates are obtained as the square root of the diagonal elements of  $C_{est}$ . We call this approach the inversion analysis.

The posterior covariance matrix is a product of an iterative, damped least-squares inversion approach (Menke, 1989) where the model update at the  $n$ th iteration is given by

$$m_{n+1} = m + [G_n^T C_{obs}^{-1} G_n]^{-1} \cdot [G_n^T C_{obs}^{-1} (d_{obs} - g(m_n))] \quad (2)$$

where  $m$  is the model vector consisting of the logarithm of the model parameters,  $d_{obs}$  is the field data vector,  $g(m)$  is the non-linear forward response vector of model  $m$ .

The model resolution matrix is defined as:

$$R = G^{-g} G \quad (3)$$

where  $G^{-g}$  is a generalised inverse to the original problem (Menke, 1989). In our case we have:

$$\begin{aligned} G^{-g} &= [G^T C_{obs}^{-1} G]^{-1} G^T C_{obs}^{-1} \Rightarrow \\ R &= [G^T C_{obs}^{-1} G]^{-1} G^T C_{obs}^{-1} \cdot G = I \end{aligned} \quad (4)$$

and the model resolution matrix is therefore not interesting as a means to appraise the solution.

Analyses are carried out on the logarithm of the model parameters:  $\log(\text{resistivity})$  and  $\log(\text{thickness})$ , and provide estimates of the absolute uncertainty the logarithms, i.e. we get the estimates (in a statistical sense)

$$\log(p) - \Delta \log(p) < \log(p) < \log(p) + \Delta \log(p), \quad (5)$$

or equivalently

$$p/\exp[\Delta \log(p)] < p < p \cdot \exp[\Delta \log(p)]. \quad (6)$$

Using  $\Delta \log(p) \approx \Delta p/p$ , we have for small  $\Delta \log(p)$ , approximately

$$p \times [1 - \Delta p/p] < p < p \times [1 + \Delta p/p] \quad (7)$$

and it is seen that for small uncertainties, the absolute uncertainty on the logarithm of the parameter is equal to the relative uncertainty on the parameter itself. It must be remembered that the analyses are based on a linear approximation to the *a posteriori* model covariance matrix, meaning that the uncertainty estimates can be trusted quantitatively only when they are small.

#### Derivative analysis

In Lawrie et al. (2009), the resolution capabilities of the TEMPEST, SkyTEM and VTEM systems were compared for several models assumed to be characteristic of the survey area. A measure of the sensitivity of the systems to changes in the model parameters was defined as the sum over all data of the difference between the response of a model, where one parameter has been perturbed, and the unperturbed model response, normalised with the noise of the AEM system. The sum over  $i = 1, \dots, N$  data of the derivatives of the  $i$ th response,  $r_i$ , with respect to the  $j$ th parameter,  $p_j$ , normalised with the variance of the data,  $var_d$  is given as:

$$S_j = \sum_{i=1}^N \frac{(\partial r_i / \partial p_j)^2}{var_d} \quad (8)$$

The sensitivities,  $S_j$ , are simply the diagonal elements of the  $G^T C_{obs}^{-1} G$  matrix of equation 1. The higher the value, the higher the sensitivity to changes in the  $j$ th parameter. We shall call this way of estimating the resolution the *derivative analysis*.

We compare the inversion analysis and the derivative analysis in a quantitative way by looking at their respective measures of parameter uncertainty for a series of three-layer models. We compare the posterior standard deviations of the inversion analysis calculated as the square root of the diagonal elements of  $[G^T C_{obs}^{-1} G]^{-1}$ , i.e.  $\{\text{diag}([G^T C_{obs}^{-1} G]^{-1})\}^{1/2}$ , with an 'equivalent standard deviation' measure for the derivative analysis, namely the inverse of the square root of the diagonal elements of  $[G^T C_{obs}^{-1} G]$ , i.e.  $\{\text{diag}[G^T C_{obs}^{-1} G]\}^{1/2}$ . Though they are derived from matrices that are each other's inverses, the two measures of resolution can only be expected to offer a relative comparison, i.e. we shall be able to see whether the well determined and poorly determined parameters are the same for the two measures.

#### Comparison of inversion and derivative analysis

For simplicity, we assume that we have what could be termed a 'generic' TEM system: a ground based, central loop configuration. We look at pure impulse response (the voltage response in an induction loop) and pure step response (the magnetic field) data in the interval from  $10 \mu\text{s}$  to  $10 \text{ms}$  not taking repetition, waveform or filtering into account; and we assume that we have a relative noise of 5% on all data. For 1D

earth models, most TEM systems (ground based or airborne) have quite similar sensitivity distribution with depth. Thus our analysis will have general validity for systems capable of collecting good data in the delay time interval  $10 \mu\text{s}$ – $10 \text{ms}$ .

We consider a series of three-layer models as seen in Table 1. The resistivity of the first and third layer are kept constant at  $10 \Omega\text{m}$  as is the thickness of the first layer at a value of 10 m. The resistivity and thickness of the second layer varies in 21 steps over two decades. The series of models have been constructed to cover both minimum and maximum models so that we should encounter two types of well known equivalence for TEM methods: (1) the low resistivity equivalence, where the parameters of a thin conductive layer cannot be determined because models with the same conductance of the second layer have very similar responses; and (2) the inability of TEM methods to distinguish between high resistivities, i.e. resistivities above a couple of hundred  $\Omega\text{m}$  (Sharma and Kaikkonen, 1999). In Figure 1, colour coded templates of the two analyses of parameter standard deviation defined above are shown for all model parameters, resistivities and thicknesses, as a function of the thickness of the second layer varying from 1 to 100 m on the abscissa and the resistivity of the second layer varying from 1 to 100  $\Omega\text{m}$  on the ordinate. Parameters with a small posterior relative standard deviation are shown in red to orange colours and parameters with a large posterior relative standard deviation are shown in green to blue colours.

We first compare the two analysis methods for impulse responses. To make the two comparable, the values of the derivative analysis have been multiplied with a factor of 2.166. This factor ensures that the two analysis types have the same average standard deviation for the resistivity of the third layer (see Table 2). This parameter is chosen as the scaling parameter because both analysis types indicate that it is well determined for almost all the models considered and that the covariance (as estimated from  $C_{est}$ , equation 1) with other model parameters is small. In the following we shall adopt the same criteria for selecting the scaling parameter: that the uncertainties are small, that the covariance with other parameters is minimal and that the uncertainties vary as little as possible over the models considered. In this way we believe that we will introduce the smallest bias in the comparison. In Table 2, we give the sum of standard deviations over all 441 models for the impulse and step responses for both inversion and derivative analysis.

We see from the templates that for impulse responses the two analysis methods agree for the well determined resistivities of the first layer – and self evidently for the third layer that was used as the scaling parameter. However, for the resistivity and thickness of the second layer and the thickness of the top layer they differ considerably: the derivative analysis displays much lower values than the inversion analysis. This is due to the fact that the derivative analysis does not take the coupling between parameters into account; it expresses the total sensitivity to changes in a certain parameter under the assumption that all other parameters remain unchanged. Mathematically, the derivative analysis comes from the diagonal elements of the

**Table 1. The parameter intervals of the three-layer models used in the comparison between the inversion analysis and the derivative analysis.**

Layer number	Resistivity ( $\Omega\text{m}$ )	Thickness (m)
1	10	10
2	1–100	1–100
3	10	

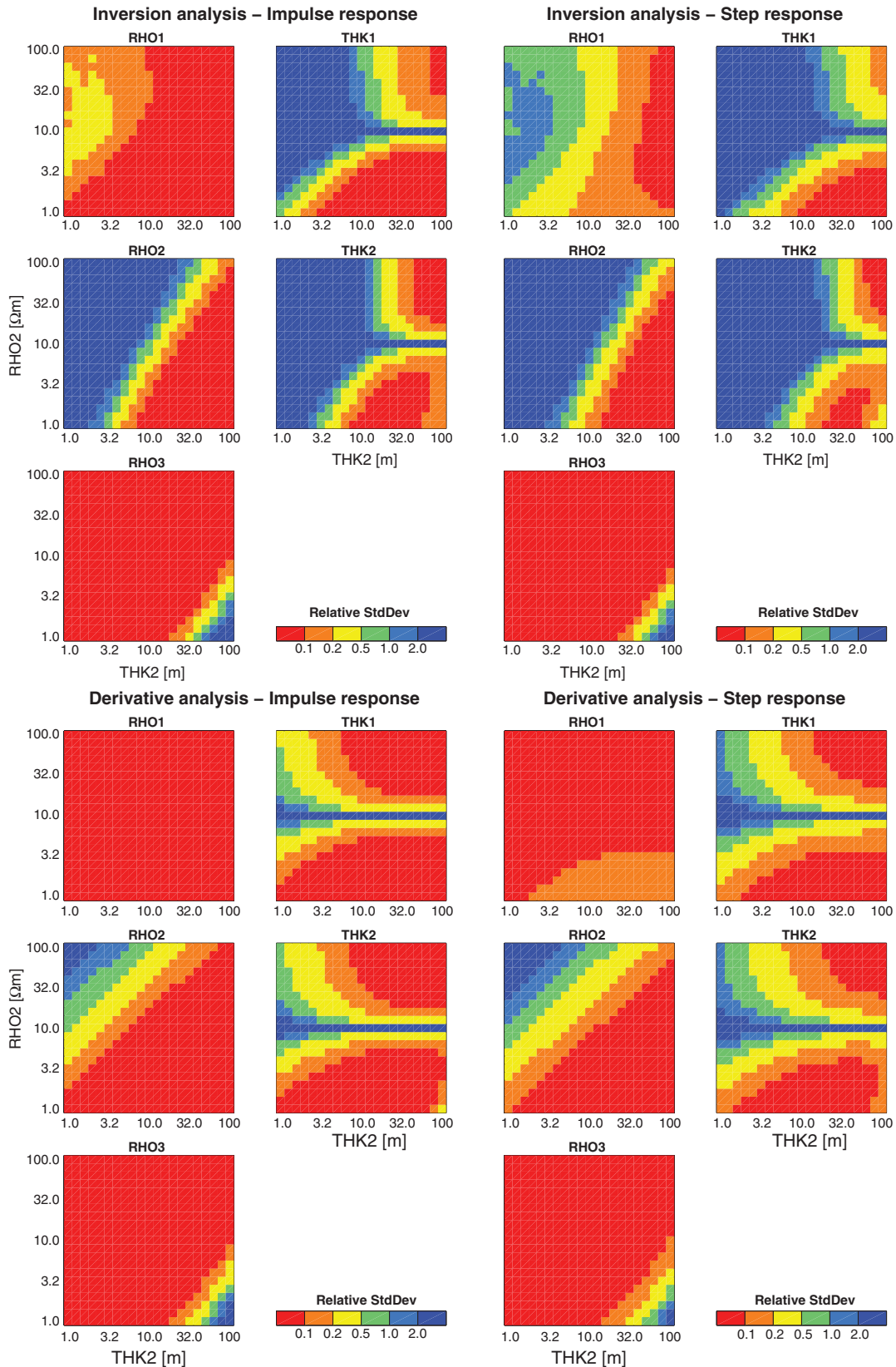


**Fig. 1.** Each of the colour coded templates shows the standard deviation of the logarithm of one of the model parameters as a function of the thickness and resistivity of the second layer. To the left are the standard deviations for the inversion analysis and to the right are the equivalent measures for the derivative analysis. The top row is for impulse responses while the bottom row is for step responses.

$[G^T C_{obs}^{-1} G]$  matrix, but the inversion model and the posterior estimate of its uncertainty comes from inverting the whole  $[G^T C_{obs}^{-1} G]$  matrix, also the off-diagonal elements. The fact

that the derivative analysis does not reflect parameter coupling is most clearly demonstrated by looking at models where there is a pronounced equivalence, i.e. a strong coupling between

**Table 2. The sum over all 441 models of the standard deviations of the inversion analysis and the derivative analysis for both impulse and step responses. The numbers used in the normalisation of the derivative analyses are shown in bold.**

Analysis method/data type	Rho1	Rho2	Rho3	Thk1	Thk2
Inversion-impulse	42.55	9965	48.31	5340	11052
Derivative-impulse	7.200	56.37	22.31	1294	1499
Ratio: Inv/Deriv	5.91	176.8	<b>2.166</b>	4.13	7.37
Inversion-step	201.9	13434	38.49	9647	14598
Derivative-step	9.306	59.80	10.57	1581	1578
Factor Inv/Deriv	21.7	224.6	<b>3.64</b>	6.1	9.186
Ratio: Inversion step/Imp	4.75	1.35	0.80	1.81	1.31

parameters. The low resistivity equivalence for layers of low resistivity and small thickness, which are found in the models in the lower left part of the templates for RHO2 and THK2, is clearly reflected in the fact that the model parameters of the second layer are undetermined in the inversion analysis. In the derivative analysis, they erroneously appear to be well determined. Also, the inability of TEM methods to distinguish between high resistivities is reflected in the upper left-hand corner of the templates for RHO2. Additionally, in this case, the derivative analysis overestimates the resolution. In the upper left-hand corner of the template for THK2 where THK2 is large, it is seen that the resolution of the thickness of the second layer is rather independent of the actual resistivity of the second layer – as should be expected. This behaviour is not seen in the derivative analysis. From the fact that the derivative analysis does not demonstrate the inherent characteristics of the equivalences of TEM methods, we conclude that the inversion analysis is preferable.

In subsequent sections of this paper we compare the SkyTEM system, which basically is an impulse response system, with the TEMPEST system which measures as an impulse response system, but for which data are deconvolved to step responses. For the sake of later argument we therefore also compare the resolution capability of impulse and step responses. In Figure 1, templates for the inversion and derivative analyses are also plotted for the step response. Again we use the resistivity of the third layer as the scaling parameter, and the derivative analysis values have been multiplied with a factor of 3.64 to make the analyses comparable.

Comparing the inversion analysis to the derivative analysis for the step response, we see a situation similar to the one for impulse response: the two analyses give similar results for well determined, uncoupled parameters - but the coupling between parameters characteristic of the TEM method is not reflected in the derivative analysis. Again, the inversion analysis is superior in that it faithfully reproduces well known limitations of TEM systems, while the derivative analysis does not.

Comparing the inversion analyses of impulse and step responses, we see that the step response has an inferior resolution of surface conductivity for all models. The resistivity of the first layer, RHO1, is well determined in the impulse response case, but this parameter is poorly determined in the case of step responses, especially when the thickness of the second layer is small. Closer inspection of the templates for the other parameters reveals that the standard deviation of the step response is slightly worse for all parameters except for the resistivity of the bottom layer where the step response gives a slightly smaller standard deviation. This is seen as a small translation to the right of the colour patterns of the templates.

For the derivative analysis, a similar situation is observed, but compared with the impulse response, the step response shows only a slightly worse resolution.

The explanation we offer for the poorer resolution of step response data is that, at very early times, the step response – being almost equal to the primary field – does not depend on the surface conductivity, while the impulse response is inversely proportional to the surface conductivity. Only at intermediate delay times will the step response reflect the near-surface conductivity and, for those delay times, the diffusion depth may be considerably greater than the thickness of the first layer with the consequence that near-surface resolution is reduced.

We emphasise that the comparison between impulse and step response systems made in this section is between systems of the same, quite compact, geometry. As mentioned above, in subsequent sections we compare the SkyTEM system, an impulse response system with a compact geometry, with the TEMPEST system, a step response system through the data processing, which has an extended geometry, and one of our findings is that the SkyTEM system, overall, will determine most model parameters better than the TEMPEST system. In an attempt to understand why, we conducted analyses for an imaginary step response SkyTEM system and for an imaginary TEMPEST impulse response system to find out whether it was the compact geometry of the SkyTEM system or the fact that it was an impulse system that gave it the edge over the TEMPEST system. The answer to that question is that – without any qualifications – it is the step response character and not the extended geometry that causes the poorer resolution. Naturally, we cannot show all these analyses in the limited space of a journal paper, but to be able to make this very important point clear, we included the comparison between impulse and step response for the generic TEM system above.

Another interesting question is to which degree the above conclusions reached under the assumption of pure step and pure impulse responses will hold up when we include the system response, i.e. the effects of repetition, waveform, low-pass filters and gating. We have not conducted an extensive analysis of this question, but we expect that if the system response is not too dominating, the above conclusions will stand. However, in the analyses to follow, the full system response of the SkyTEM system is included in the comparison with the TEMPEST system. Except for the repetition, the TEMPEST system response is removed in the data processing deconvolving the measured impulse response into a step response.

## Comparative analyses using five-layer models

### Noise models

It is clear from equations 2 and 8 that both the derivative and inversion analyses depend critically on the noise level. It is therefore important for the reliability of the uncertainty estimates that the noise model adequately describes the real measuring situation. In this section we compare the resolution capability of the two TEM systems selected as candidates for the survey: the SkyTEM and TEMPEST systems, using both the inversion and the derivative analyses. Before showing results of the comparison we take a closer look at the noise models used to describe the properties of the systems.

In the official GA noise model for airborne EM systems (Lawrie et al., 2009), the noise is described as consisting of three contributions: (1) a bias signal, (2) an additive noise and (3) a multiplicative noise. For each gate, the bias signal is determined as the mean of the gate value for a high altitude

measurement, the additive noise is the standard deviation on the bias. The multiplicative noise is a measure of the repeatability of the data determined through repeated flights over the same test line and is given as an average value over all gates.

GA obtains noise estimates from the contractors involved in their surveys and keeps them for reference and use in future analyses. Additionally, GA estimates noise characteristics from repeat line data and high altitude measurements, independent of the contractor. Before undertaking the comparative analysis, we made sure that the noise models were current. As a result, an updated SkyTEM noise model was obtained from the Hydrogeophysics Group at the University of Aarhus, Denmark, who manage the calibration of the SkyTEM system for the Danish contractors (Foged et al., 2010). In this noise model, bias is much smaller than the additive noise and can be neglected. The TEMPEST noise model on file at GA needed no updating. Only the vertical component of the data is used in this study and the noise models for bias and additive noise for the SkyTEM and TEMPEST systems are shown in Figure 2. In the conductive environment of the survey area, it was stipulated that data with a good signal to noise ratio might be achieved up to a delay time of 20 ms. The SkyTEM noise model was given for delay times only up to 10 ms, so the noise values were extrapolated to 20 ms as seen in Figure 2. The multiplicative noise is 1.5% and 1.7% for the SkyTEM and TEMPEST systems, respectively.

As seen in Figure 2, there are separate estimates of the additive noise for the low and the high moment of the SkyTEM system and in a loglog plot the noise amplitudes decrease with delay time approximately with a slope of  $-1/2$ . These estimates are in accordance with the expected behaviour of averaging random noise over gates with widths increasing proportionally with delay time. The TEMPEST noise estimates do not display this behaviour; they appear rather constant with delay time. This

must be attributed to the deconvolution of the measured data into a 100% duty cycle step response routinely performed on TEMPEST data. The methodology of producing the noise estimates is described in Green and Lane (2003). While the bias and additive noise definitions are fairly straightforward, the multiplicative noise contribution is more complicated. Navigation errors, varying height and the character of the sensitivity function, especially its lateral extent, influence the multiplicative noise estimate. In Green and Lane (2003), navigation errors are dealt with by resampling, and an approximate height correction is applied to the measured data.

Because of the multiplicative part of the noise model, the noise to be ascribed to the data depends on the data value, so a model response needs to be calculated for each model. The total relative noise is then calculated as

$$\Delta_{rel}d = \frac{\sqrt{(m \cdot d)^2 + b^2 + a^2}}{d}, \quad (9)$$

where  $d$  is the model response,  $m$  is the multiplicative noise,  $b$  is the bias and  $a$  is the additive noise. In this formulation it is assumed that the three contributions to the noise are independent and log-normal distributed.

#### The data

The data used in this report are theoretical data based on forward responses of the representative models to be analysed. After responses are calculated, noise is ascribed according to equation 9 using the parameters of the noise model. In the forward calculation and inversion analysis, the full system characteristics of the SkyTEM system are taken into account. The TEMPEST system measures the rate of the change of the magnetic field components in receiver coils from a step-like source, but data are deconvolved into 100% duty cycle step responses – and consequently, this is the data type modelled in this study. The recording parameters of the SkyTEM and TEMPEST systems are shown in Tables 3 and 4; the gate information of the TEMPEST system refers to the deconvolved data.

#### The models

The five-layer models in Table 5 comprise most of the models analysed in Lawrie et al. (2009). Model parameters are fixed except for the resistivities of the second and third layers. The resistivity of the second layer varies over a decade from 1 to 10  $\Omega\text{m}$  while the resistivity of the third layer varies from 0.5 to 50  $\Omega\text{m}$ , both in 21 steps giving 441 different models. All layer resistivities are quite low except for certain values of the third layer, so it must be expected that depth penetration will be limited. For some of the models, resistivity contrast between

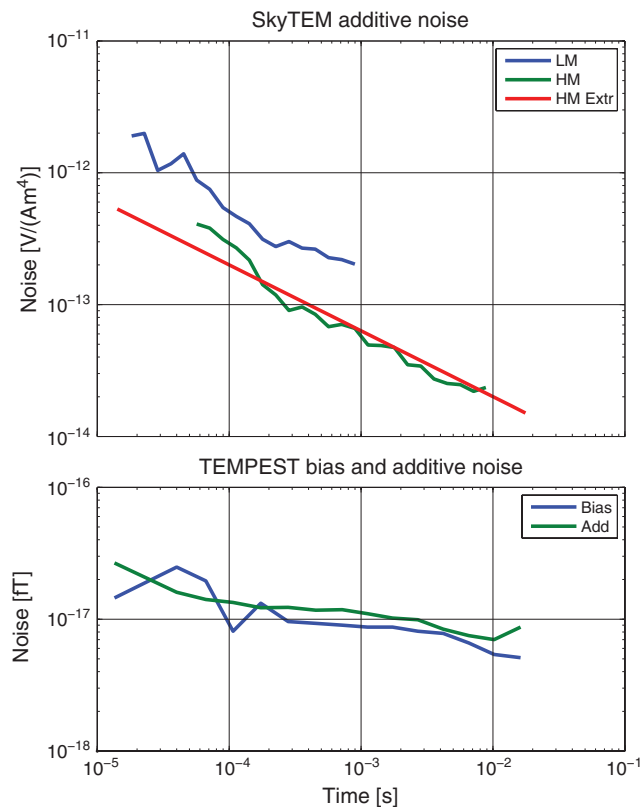


Fig. 2. Bias and additive noise for the SkyTEM and TEMPEST systems.

Table 3. Recording parameters of the SkyTEM system.

Configuration parameter	Low moment	High moment
Tx area	314 m <sup>2</sup>	314 m <sup>2</sup>
Rx cut-off frequency	450 kHz	450 kHz
Amplifier filter	100 kHz	100 kHz
Front gate	13.5 $\mu$	59.5 $\mu$
Receiver sampling frequency	N/A	N/A
Gate centre time of first gate	17.2 $\mu$	180 $\mu$
Gate centre time of last gate	1.13 ms	17.9 ms
Repetition frequency	222 Hz	12.5 Hz
Transmitter altitude	35 m	35 m
Receiver altitude	37.1 m	37.1 m
Horizontal Tx-Rx separation	10.61 m	10.61 m

**Table 4. Recording parameters of the TEMPEST system.**

Configuration parameter	Value
Tx area	186 m <sup>2</sup>
Rx cut-off frequency	unknown
Amplifier filter	unknown
Front gate	none
Receiver sampling frequency	75 kHz
Gate centre time of first gate	13 $\mu$
Gate centre time of last gate	16.2 ms
Repetition frequency	25 Hz
Transmitter altitude	120 m
Receiver altitude	78 m
Horizontal Tx-Rx separation	120 m

**Table 5. Parameters of the test models.**

Layer #	Thickness (m)	Resistivity ( $\Omega$ m)	Lithology
1	10	1.6	Coonambidgal formation
2	15	1.0–10	Shepparton formation, silty sand
3	50	0.5–50	Calivil sand
4	50	3	Upper Renmark Group, silty sand
5		5	Middle and lower Renmark Group, silty sand

neighbouring layers is low, resulting in a poor determination of the layer boundary.

### The analyses

In Figures 3, 4 and 5, analyses of the resistivities (RHO), thicknesses (THK) and depths (DEP), respectively, are presented as coloured pixels in templates. Each template shows the relative uncertainty of one of the model parameters as a function of the resistivity of the second layer (the abscissa) and the resistivity of the third layer (the ordinate). The colour indicates the relative uncertainty of the model parameter in six levels, red being the lowest uncertainty and blue the highest. To further illuminate the difference between the inversion analysis and the derivative analysis and to see if the ranking of the two systems is the same for the two analysis methods, both types of analyses are presented in these figures.

In Figures 4 and 5, for the SkyTEM system, a vertical blue line, corresponding to unresolved parameters, appears where  $RHO2 = RHO1 = 1.6 \Omega$ m. This happens when parameter resolution depends on a resistivity contrast between the first and second layer, e.g. for THK1, THK2 and DEP1. This line is not seen in the corresponding inversion analyses of the TEMPEST system because all the models in the templates are undetermined. In the corresponding derivative analyses the vertical line is absent which further illustrates that the coupling between model parameters does not show up in the derivative analyses.

In Figures 4 and 5, for the SkyTEM system, a horizontal blue line, corresponding to unresolved parameters, appears where  $RHO3 = RHO4 = 3 \Omega$ m. This happens when parameter resolution depends on a resistivity contrast between the third and fourth layer, e.g. for THK3, THK4 (not visible because THK4 is undetermined for all parameters) and DEP3. This line is not seen in the corresponding inversion analyses of the TEMPEST system because all the models in the templates are undetermined. In this case the line is also seen in the corresponding derivative analyses for THK3.

Likewise, a blue line with a slope of 1 is present where  $RHO2 = RHO3$  for the parameters whose resolution depends on a resistivity contrast between the second and third layer, i.e. for THK2 and DEP2. The line is seen in all analysis templates except where masked by a completely blue template.

### SkyTEM inversion analyses

The analyses of the resistivities RHO1, ..., RHO5 (cf. Figure 3) show that RHO1 is well determined for all models. RHO2 is better determined when layers 2 and 3 are conductive. RHO3 is determined when low, but not when it attains higher values. RHO4 and RHO5 are unresolved.

The analyses of the thicknesses THK1, ..., THK4 show that THK1 is reasonably well determined when RHO3 is low and best when RHO2 is low, but THK1 becomes more poorly determined when RHO3 is high. Naturally, THK1 and THK2 are unresolved when  $RHO2 = RHO1 = 1.6 \Omega$ m. THK2 is reasonably determined when RHO3 is lowest, but not for higher values of RHO3. THK3 is poorly determined when RHO3 is low and otherwise unresolved. THK4 is undetermined.

The analyses of the depths DEP1, ..., DEP4 show that DEP2 is much better determined than either of THK1 and THK2 which is common, and it is best determined for low RHO3. DEP2 is unresolved along the line where  $RHO2 = RHO3$ . DEP1 is of course the same as THK1. DEP3 is fairly well determined for low values of RHO3 and otherwise undetermined. DEP4 is unresolved.

Overall, the analyses show that only the parameters pertaining to the top 2–3 layers can be determined with low to medium uncertainty. The resistivity of the fourth and fifth layers and the thicknesses of and depths to the third and fourth layers are undetermined. This is mainly due to the low resistivities of the overlying layers and the resulting limited depth penetration.

### TEMPEST inversion analysis

The analyses of the resistivities RHO1, ..., RHO5 show that RHO1 is reasonably determined for lower values of RHO2 and RHO3, but otherwise poorly determined. RHO5 is reasonably determined for high values of RHO2 and RHO3, but otherwise poorly determined. All other resistivities and all thicknesses and depths are by and large undetermined, the exception being the resistivity of the fifth layer for which the relative uncertainty is below 0.5 for the higher values of RHO2 and RHO3. The resistivity of the fifth layer is also the only parameter for which the TEMPEST system shows better resolution than the SkyTEM system.

### Comparing the inversion and derivative analyses

To be able to compare the inversion and derivative analysis, we have normalised the derivative analyses as in the generic system comparison (cf. Figure 1). We demand the same average uncertainty in the derivative analysis as in the inversion analysis of RHO1 for the SkyTEM analyses. This is the only parameter fulfilling the criteria of being well determined by both the SkyTEM and TEMPEST systems and being only weakly coupled to other parameters.

Comparing the inversion and derivative analyses for the resistivities and thicknesses, the same tendency is seen as in the generic system analyses: the derivative analysis generally overestimates the resolution capability. Comparing the derivative analyses for the resistivities for the SkyTEM and TEMPEST systems, we see that the two systems are more

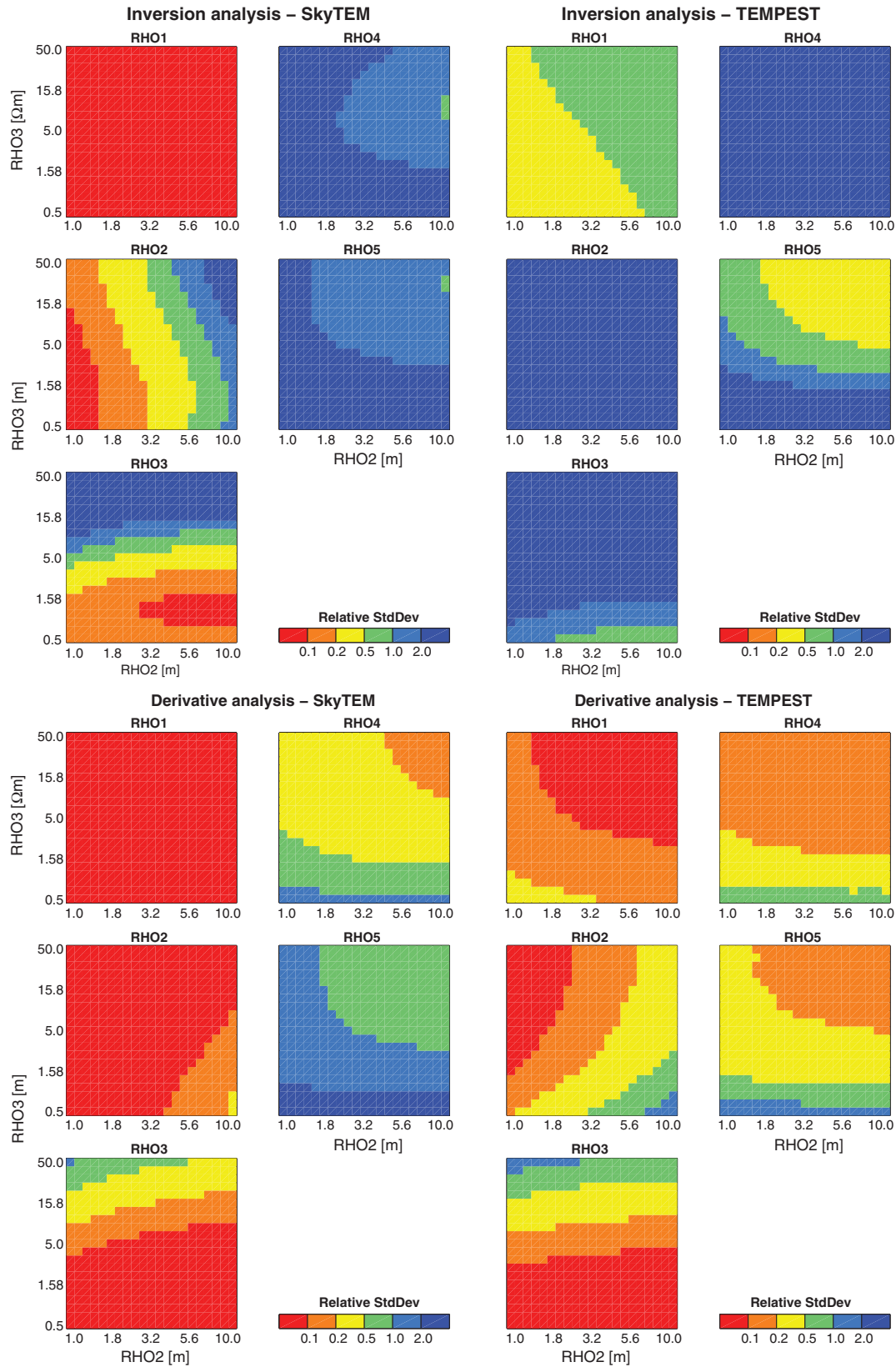


**Fig. 3.** Analysis templates for layer resistivities. SkyTEM (left column) and TEMPEST (right column); inversion analysis (top row) and derivative analysis (bottom row). Derivative analyses are scaled to fit the posterior analysis for RHO1 for SkyTEM.

similar in the derivative analysis than in the inversion analysis. It is also worth noting that the derivative analyses gives the two systems a similar resolution of RHO3, while the TEMPEST system is better at resolving RHO4 and RHO5.

The same general pattern is seen concerning the derivative analyses of the thicknesses as for the resistivities: the derivative analysis generally overestimates the resolution capability. Also, for the thicknesses, it is seen that the

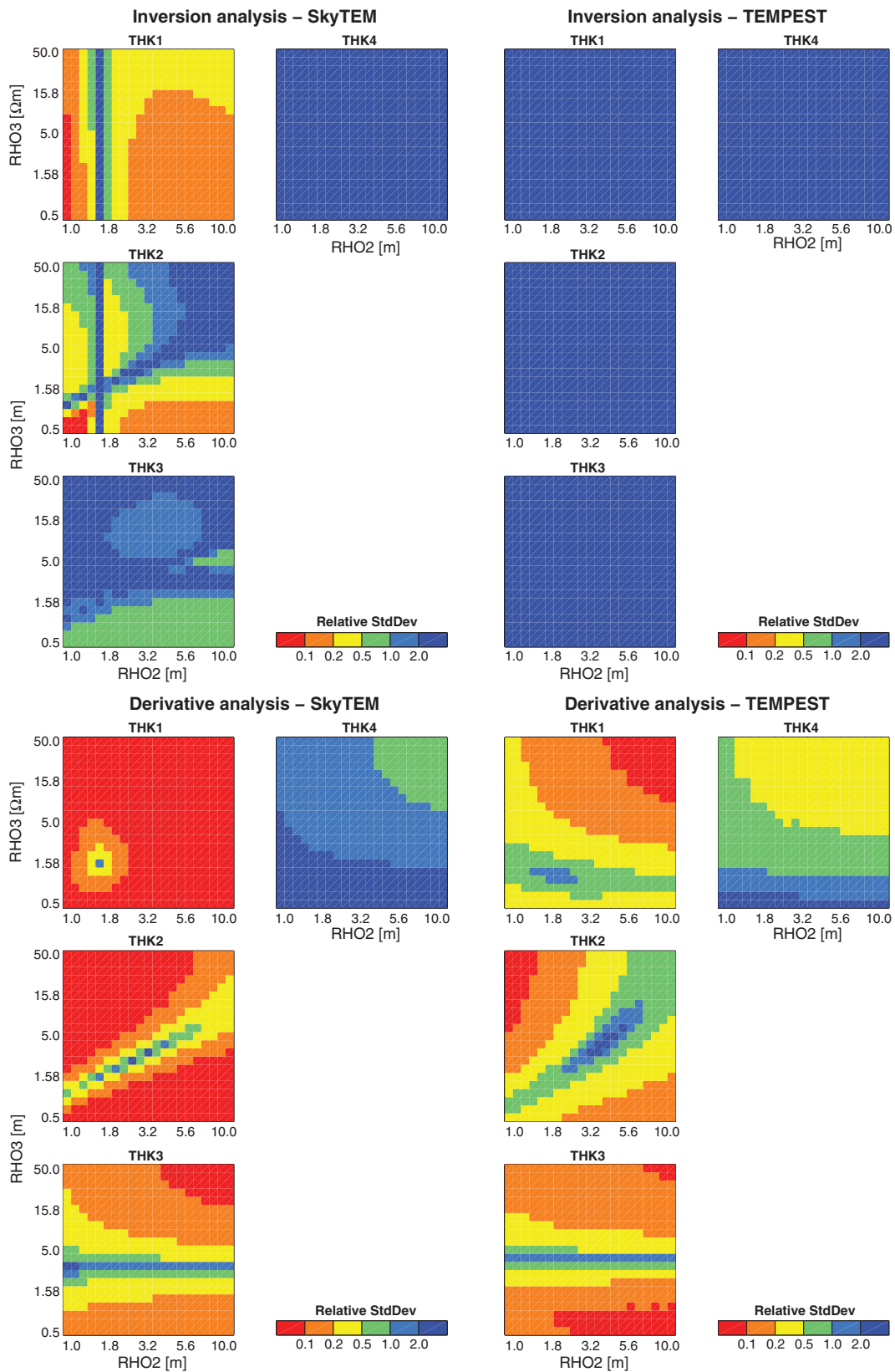


**Fig. 4.** Analysis templates for layer thicknesses. SkyTEM (left column) and TEMPEST (right column); inversion analysis (top row) and derivative analysis (bottom row). Derivative analyses are scaled to fit the posterior analysis for RHO1 for SkyTEM.

derivative analysis puts the two systems on a more equal footing, with the TEMPEST system being superior for the deeper parameters.

**Comparison of multi-layer inversions**

Although the above analyses show that several of the model parameters cannot be determined well by either of the two

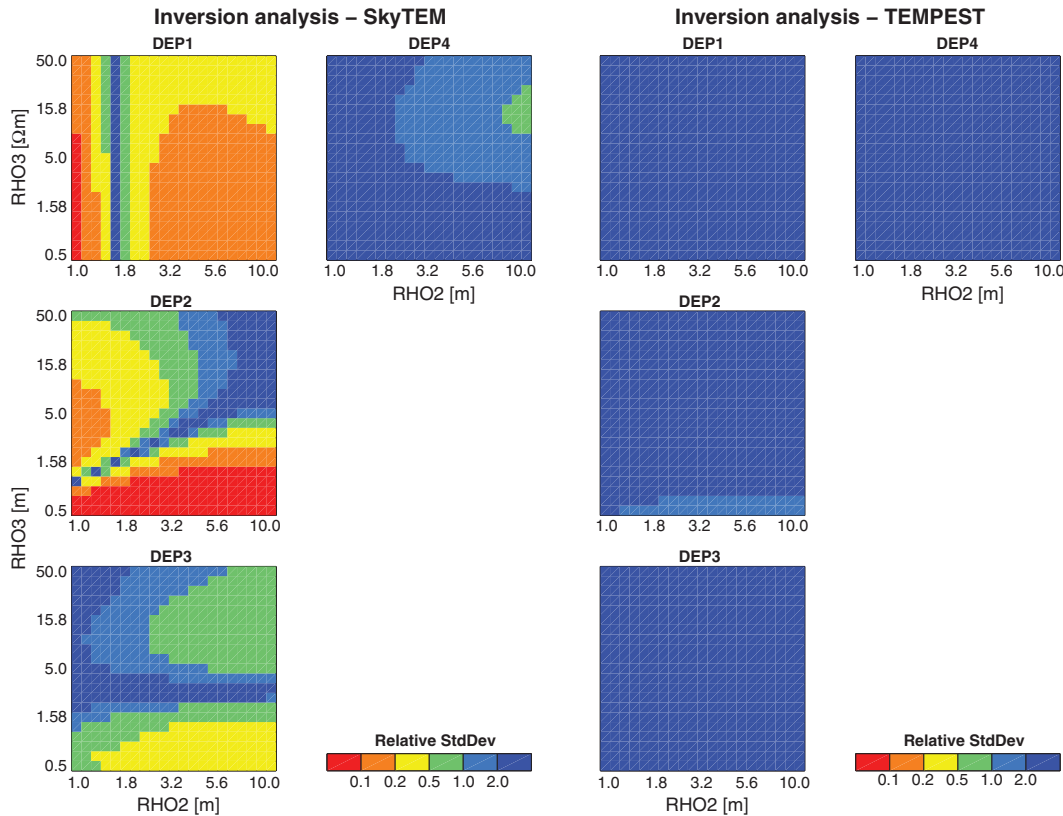


Fig. 5. Analysis templates for the SkyTEM (left) and TEMPEST (right) systems for the depth to layer boundaries.

systems, subtle differences in resistivity might still be visible in multi-layer inversion of the data from the five-layer models. Even if not *resolved*, resistivity variations may be *indicated*. To investigate this, the forward responses from the five-layer models, statistically perturbed with noise according to the noise models, are inverted with 30-layer models.

The inversion is carried out using an iterative, damped least-squares inversion approach (Menke, 1989). The model update at the  $n$ th iteration is given by

$$m_{n+1} = m_n + [G_n^T C_{obs}^{-1} G_n + C_m^{-1}]^{-1} \cdot [G_n^T C_{obs}^{-1} (d_{obs} - g(m_n)) + C_m^{-1} (m_{prior} - m_n)] \quad (10)$$

where the inversion is regularised through the use of a broadband covariance matrix,  $C_m$ , that essentially contains all correlation lengths and ensures vertical smoothness of the inversion result (Serban and Jacobsen, 2001; Christensen et al., 2009). For an explanation of the other symbols, we refer to equation 1.

The results are shown in Figures 6, 7 and 8, each showing inverted models for constant RHO3 and varying RHO2 along the profile. We present model series for three different values of RHO3 out of the 21 analysed: RHO3 = 0.792, 1.58 and 7.92  $\Omega\text{m}$ . For all models, the resistivities of the fourth and fifth layers are kept constant, equal to 3  $\Omega\text{m}$  and 5  $\Omega\text{m}$ , respectively. The initial model for all inversions is a homogeneous halfspace with a resistivity of 5  $\Omega\text{m}$  and the vertical regularisation is the same for both SkyTEM and TEMPEST. All inversion models in all three figures converged to fit the data well. In Figures 6, 7 and 8, three model sections are displayed: the true models, the model section from inverting SkyTEM data, and the model section from inverting TEMPEST data.

To avoid misunderstandings, we emphasise that the model series of Figures 6, 7 and 8 are not model sections in the traditional sense; each model is inverted individually and there are no lateral smoothness constraints. In real field situations, the noise-affected data would be processed to reduce data noise and to discard invalid data. We have not had access to the proprietary data processing schemes for neither SkyTEM nor TEMPEST data and we have not processed data in any way. For this reason, and the fact that the inversions are done individually for each model without any lateral constraints, the models appear more erratic than they would in a real field situation. The erratic behaviour is more pronounced for the SkyTEM than the TEMPEST system because the noise is slightly higher on the SkyTEM data.

In Figure 6, for RHO3 = 0.792  $\Omega\text{m}$ , the conductive upper layer, the second layer which varies from conductive to resistive, and the third rather thick conductive layer are well distinguished from one another by the SkyTEM system. There is a tendency for the conductivity of the third layer to be slightly overestimated. The TEMPEST inversions show the same general features, but for the upper three layers, they are not so clearly distinguished from one another as for the SkyTEM system and there is a tendency for the conductivity of the upper layer to be overestimated. However, the higher resistivities of the fourth and fifth layers are best indicated by the TEMPEST system.

In Figure 7, for RHO3 = 1.58  $\Omega\text{m}$ , the top three layers can still be distinguished in the SkyTEM section. The TEMPEST model section has become considerably more blurred than the previous one. None of the systems show any resolution at depth.

In Figure 8, for RHO3 = 7.92  $\Omega\text{m}$ , the third layer is now relatively resistive. The SkyTEM section is capable of defining the top layer and to indicate the second layer where it is

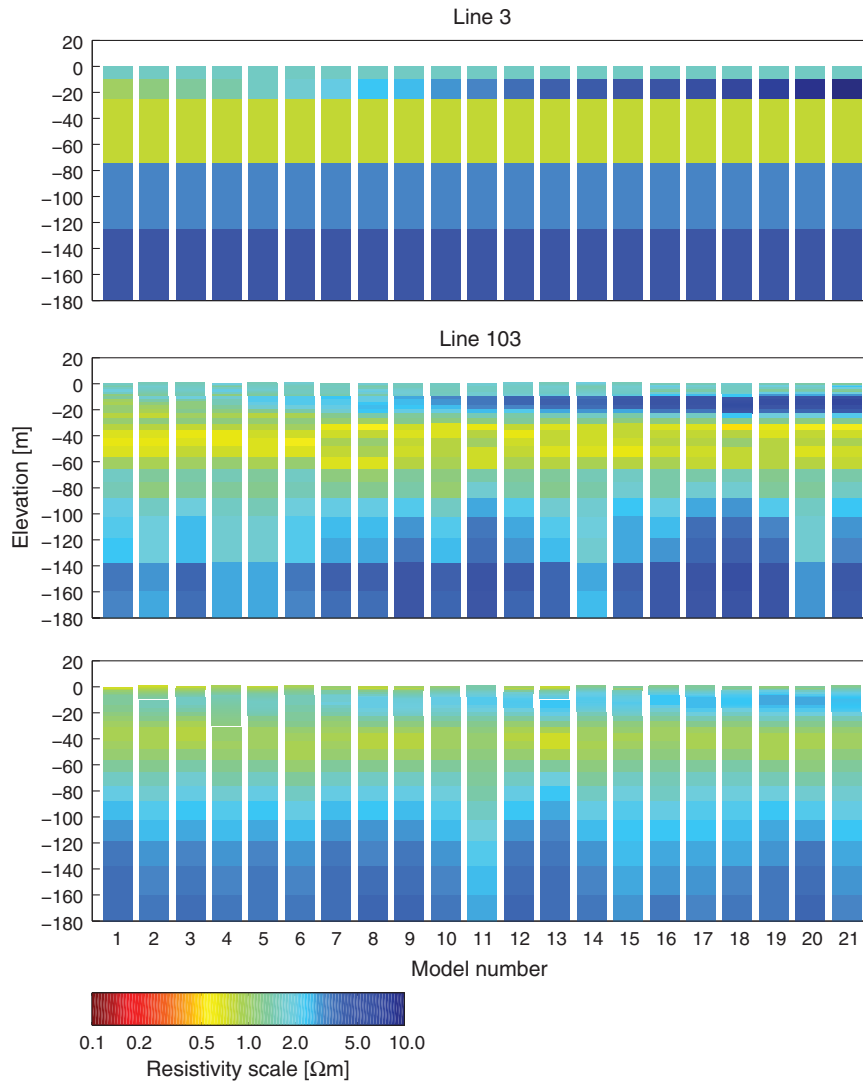


**Fig. 6.** Multi-layer inversion of noise perturbed data from the five-layer models. Top: true models; middle: SkyTEM inversion; bottom: TEMPEST inversion.  $\rho_{02}=1, \dots, 10 \Omega\text{m}$ ,  $\rho_{03}=0.792 \Omega\text{m}$ ,  $\rho_{04}=3 \Omega\text{m}$  and  $\rho_{05}=5 \Omega\text{m}$ .

conductive. The resistivity of the third layer is quite well reproduced. In the TEMPEST section, there is also a well defined top layer, and the conductive part of this can be seen; however, the top three layers cannot be clearly distinguished from one another, except that the conductive part of the second layer can be seen. The resistivity of the third layer is not as well reproduced in the TEMPEST section as in the SkyTEM section. Below the third layer, none of the systems is able to distinguish resistivity variations.

Even though the analyses of the TEMPEST system in the previous section showed poor resolution of several model parameters, the model sections of inverted data show that structure is in fact indicated. However, as expected from the analyses, in none of the above three sections can the bottom two layers be distinguished from one another by either of the two systems.

**Discussion**

The relative uncertainty of the model parameters emerging from the inversion analysis depends critically on the noise model. On average, for small uncertainties, the relative uncertainty of the model parameters scales with the noise level: twice the noise,

twice the relative uncertainty. It is thus critical that the noise model can be trusted to give a fair picture of the system performance. This, however, is not a trivial matter and several issues are important, both in the analysis of the resolution capability of one system, and – even more so – in a comparative analysis of several systems.

The first issue is that the so-called ‘noise levels’ of the different systems are either based on information from the contractors and system manufacturers or on typical survey results obtained in comparative surveys. In principle, it is possible to obtain a noise level as small as one wishes. The more heavy-handed the processing, the more averaging, the ‘better’ the signal to noise ratio. Almost all of the data processing procedures applied by contractors are proprietary information and not divulged to the client; it is a matter of trust whether the signal-to-noise levels claimed by the contractor have been obtained in a reasonable way.

With regard to the data processing of the TEMPEST system, some additional reflections are appropriate concerning the deconvolution processing of the data. The TEMPEST system, like most other systems, has a step-off transmitter waveform and measures the rate of change of the magnetic field in induction

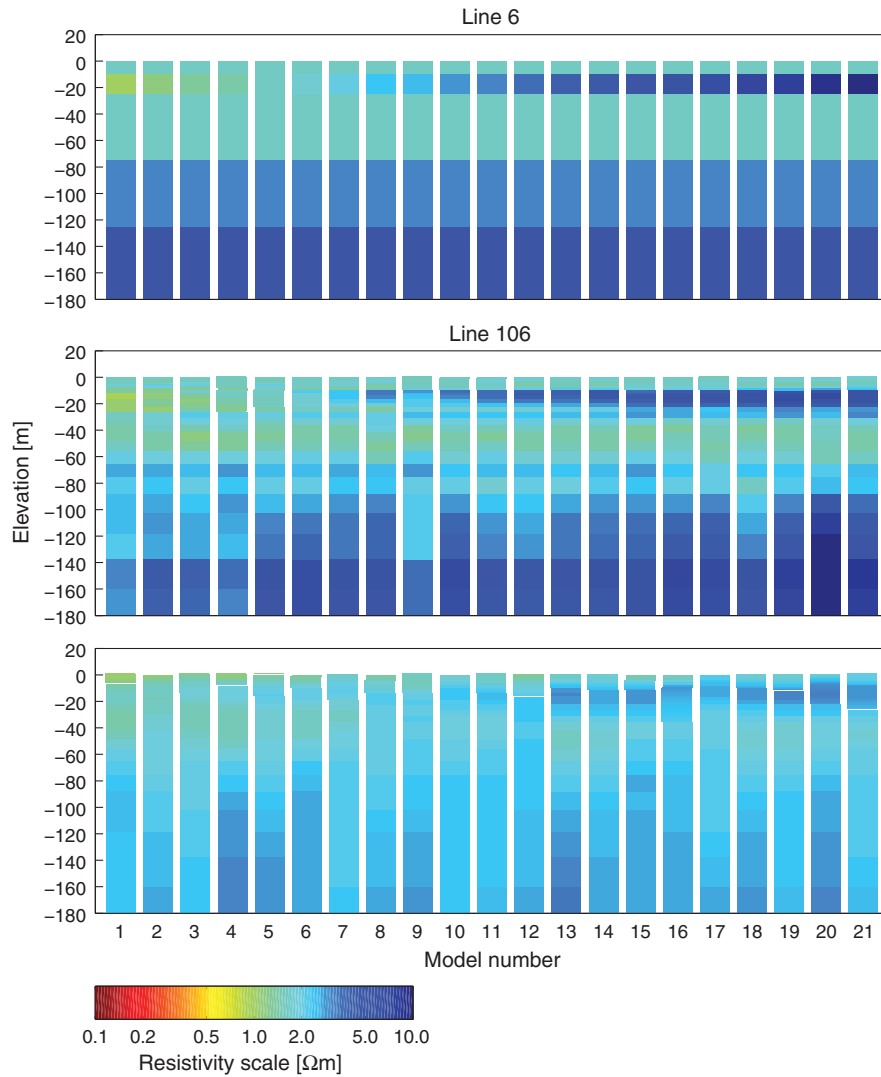


**Fig. 7.** Multi-layer inversion of noise perturbed data from the five-layer models. Top: true models; middle: SkyTEM inversion; bottom: TEMPEST inversion.  $\text{RHO2} = 1, \dots, 10 \Omega\text{m}$ ,  $\text{RHO3} = 1.58 \Omega\text{m}$ ,  $\text{RHO4} = 3 \Omega\text{m}$  and  $\text{RHO5} = 5 \Omega\text{m}$ .

receiver coils. Subsequently data are deconvolved to give a 100% duty cycle step response. However, any deconvolution requires knowledge of the input function for all frequencies, or in this case all delay times, i.e. more information than is given in the measured data, so assumptions about the early and late time behaviour of the measured signal must be made. These assumptions will have consequences for the near-surface and deep parts of the model obtained after inversion of the deconvolved data. The deconvolution introduces both late-time data between 10 ms and 20 ms delay time even though the offtime of the TEMPEST system is 10 ms, and early-time data at 13, 26 and 39  $\mu\text{s}$  even though the turnoff time of the transmitter is  $\approx 40 \mu\text{s}$ . These early- and late-time data obtained from the deconvolution thus depend on times where the transmitter was on, and consequently errors in the waveform or the position and attitude of the receiver coil will have an influence on these data. It does not seem reasonable that these data points should have the same noise as data points in the middle delay time range. Yet, that is the result of the data processing, and it is caused by the fact that a deconvolution process loses track of the noise of the individual measurements; noise becomes more or less evenly distributed over all of the deconvolved data. This is apparent

from the plot of the TEMPEST noise levels seen in Figure 2. The noise level is rather constant and does not display the physically meaningful behaviour for ambient quasi-white noise: that the noise level should decrease with a slope of around  $-1/2$  in a double logarithmic plot.

The second issue is that the accuracy of nominal system configuration parameters, e.g. system height, vertical and horizontal transmitter-receiver distance, pitch and roll of the system, residual primary field contaminating the measurement, calibration errors, system drift, etc. are often not included in the analyses. Systems differ greatly in this regard. For fixed-wing systems with a trailing bird, the receiver position relative to the transmitter varies considerably during survey, and this can also be the case for helicopterborne systems for which the transmitter-receiver geometry is not fixed. Some helicopterborne systems have a well defined geometry. The modelling errors arising from an inaccurate system description are quantified and discussed in detail in Christiansen et al. (2011) and should be included in the comparative analyses in a way similar to the ‘holistic inversion’ approach of Brodie and Sambridge (2006). In such an analysis, systems with well defined geometry and with reliable monitoring of configuration parameters would be

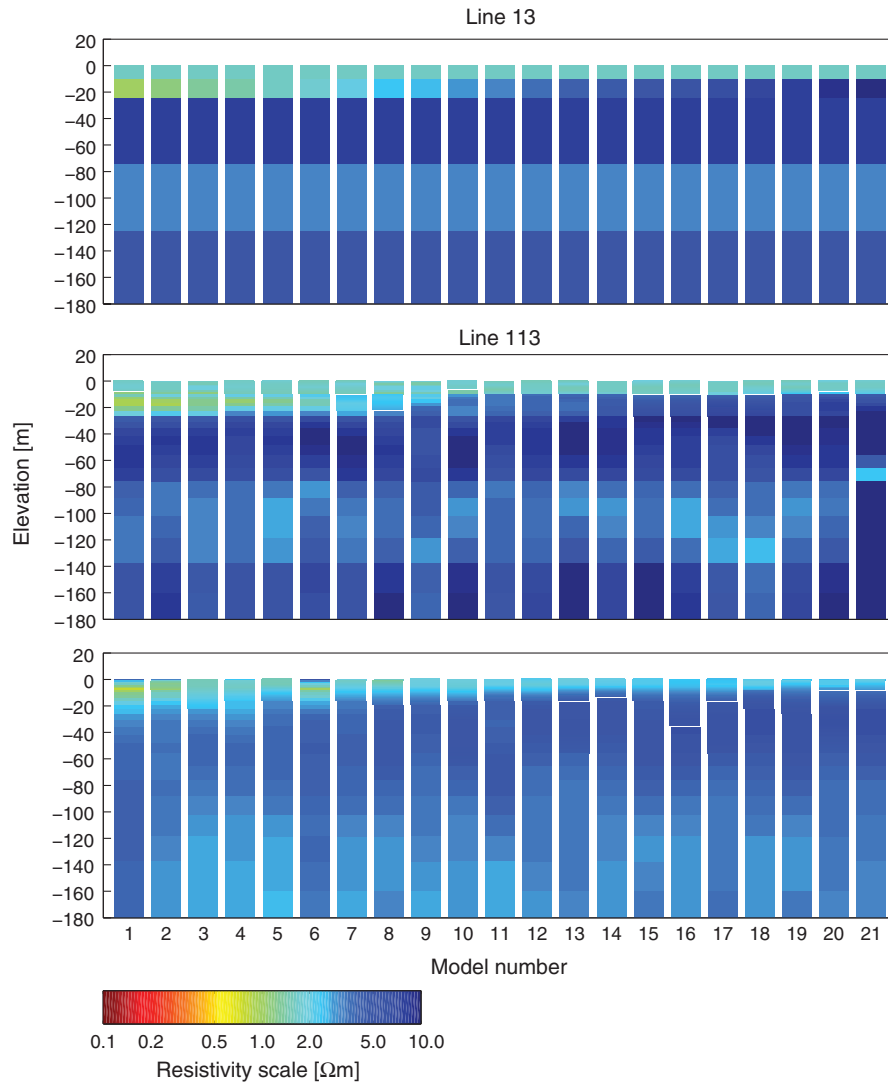


**Fig. 8.** Multi-layer inversion of noise perturbed data from the five-layer models. Top: true models; middle: SkyTEM inversion; bottom: TEMPEST inversion.  $\rho_{02} = 1, \dots, 10 \Omega\text{m}$ ,  $\rho_{03} = 7.92 \Omega\text{m}$ ,  $\rho_{04} = 3 \Omega\text{m}$  and  $\rho_{05} = 5 \Omega\text{m}$ .

favoured, as they should, while systems with variable and unmonitored geometry would be downgraded, as they should. The SkyTEM system belongs to the former category; the TEMPEST system to the latter.

The analyses presented in this paper consider only model parameters and do not take configuration parameters into account. Though we have just argued that this is an incomplete approach, our results will, by and large, reflect the resolution capability of the SkyTEM system because it is a well calibrated system with a rigid configuration for which transmitter height, pitch and roll are monitored with dual systems. For the TEMPEST system, analyses not properly taking into account the effects of the variable transmitter-receiver geometry will result in an overoptimistic picture.

A third issue is the sensitivity to lateral changes in the resistivity structure. Fixed-wing systems with long transmitter-receiver separation have a large footprint and thereby not the same early-time, near-surface lateral resolution as more compact systems. The smallest footprint, and thereby the best lateral spatial resolution, is obtained with systems with a compact geometry that are flown at low altitudes and that possess early time gates. However, beyond the evident differences in the

footprint of the systems we have compared, it is beyond the scope of this paper to go into details concerning the sensitivity functions of airborne TEM systems.

In the inversion analyses of models representative of the survey area, the TEMPEST system displayed quite poor near-surface resolution. As mentioned, this surprising result spurred the analyses presented earlier in this paper for a generic TEM system. The explanation we offer is that the poor near-surface resolution is a consequence of the fact that TEMPEST data are deconvolved to step responses. Particularly for the very conductive models analysed here, the step response will be in early-time mode for several of the early time gates and thereby not carry much information about the near-surface layers. At later times, responses become sensitive to the resistivity of the lower layers.

**Conclusions**

Though only a part of the full decision-making process, a comparative system analysis with regard to model parameter uncertainty is mandatory in a comprehensive selection process of the optimal AEM system for particular survey aims. The model

parameter uncertainty of an AEM system depends critically on the achievable signal-to-noise ratio, and the geophysicists involved in the comparative study must use their experience and general insight to evaluate whether the proprietary noise figures supplied by the contractors are reasonable or not.

It is evident that the derivative analysis does not take the coupling between parameters into account that is characteristic of the TEM method. Furthermore, the derivative analysis generally overestimates the resolution power of the TEM method - and likely any EM method. The overestimation depends on the model in general and the parameter in question in particular, and there is furthermore no guarantee that the ranking between systems will be the same using the derivative analysis as using the inversion analysis. We have in fact demonstrated that for several of the model parameters of the five-layer conceptual models for the survey area, the derivative analysis gave a different ranking between the SkyTEM and TEMPEST systems than that obtained in the inversion analysis. Ross C. Brodie, Geoscience Australia, has reported a similar behaviour in other system comparisons (personal communication). The use of the derivative analysis method may thus result in a suboptimal choice of AEM system. We do not hesitate to conclude that the inversion analysis is distinctly superior to the derivative analysis and that the latter should be considered obsolete.

Impulse and step response systems are not equivalent in practice. The near-surface resolution of step response data is inferior to that of impulse response data because, at very early times, the step response does not depend on the surface conductivity while the impulse response is inversely proportional to the surface conductivity. Only at intermediate delay times does the step response reflect the near-surface conductivity and for those delay times, the diffusion depth may be considerably greater than the thickness of the first layer with the consequence that near-surface resolution is lost. Our analysis of the generic TEM system shows that there is a difference between step and impulse systems for the same Tx-Rx geometry. We must therefore emphasise that it is not the extended geometry of the TEMPEST system that causes problems with the near-surface resolution; it is the fact that it - through the applied data processing scheme - provides step and not impulse response data.

In our analyses of the resolution capability of the SkyTEM and TEMPEST systems with regard to the five-layer models typical for the survey area, the SkyTEM system has the better near-surface resolution and both systems were incapable of mapping the deeper layers with any certainty.

### Disclosure of interests

NBC has been involved in the development of the SkyTEM system on the sideline, mainly as a sparring partner for Kurt Sørensen, the main developer of the system. NBC has also been a consultant of both SkyTEM Aps, Denmark, and Fugro Airborne Services Pty Ltd, Perth, Western Australia, developing inversion procedures for airborne EM data.

### Acknowledgements

The present work was conducted under a collaboration agreement between Geoscience Australia and University of Aarhus. Discussions with Ross C. Brodie, Geoscience Australia, were greatly appreciated. Aaron Davis and Yusen Lee-Cooper are thanked for their remarks to the first drafts, and Anders Vest Christiansen and an anonymous reviewer are thanked for their thorough and constructive reviews that definitely improved the paper.

### References

- Baumgartner, F., and Christensen, N. B., 1998, Analysis and application of a non-conventional underwater geoelectrical method in Lake Geneva, Switzerland. *Geophysical Prospecting*, **46**, 527–541. doi:10.1046/j.1365-2478.1998.00107.x
- Brodie, R., and Sambridge, M., 2006, A holistic approach to inversion of frequency-domain airborne EM data. *Geophysics*, **71**, G301–G312.
- Brown, V., Hoversten, M., Key, K., and Chen, J., 2012, Resolution of reservoir scale electrical anisotropy from marine CSEM data. *Geophysics*, **77**, E147–E158.
- Christensen, N. B., 2000, Difficulties in determining of electrical anisotropy in subsurface investigations. *Geophysical Prospecting*, **48**, 1–19. doi:10.1046/j.1365-2478.2000.00174.x
- Christensen, N. B., and Dodds, K., 2007, Special section: marine controlled-source electromagnetic methods. 1D inversion and resolution analysis of marine controlled-source EM data. *Geophysics*, **72**, WA27–WA38.
- Christensen, N. B., and Sørensen, K. I., 2001, Pulled array continuous electrical sounding with an additional inductive source. An experimental design study. *Geophysical Prospecting*, **49**, 241–254. doi:10.1046/j.1365-2478.2001.00257.x
- Christensen, N. B., Reid, J. E., and Halkjaer, M., 2009, Fast, laterally smooth inversion of airborne transient electromagnetic data. *Near Surface Geophysics*, **7**, 599–612. doi:10.3997/1873-0604.2009047
- Christiansen, A. V., and Auken, E., 2010, A global measure for depth of investigation in EM and DC modelling: *Extended abstracts of the ASEG meeting, Sydney 2010*.
- Christiansen, A. V., and Christensen, N. B., 2003, A quantitative appraisal of airborne and ground-based transient electromagnetic (TEM) measurements in Denmark. *Geophysics*, **68**, 523–534.
- Christiansen, A. V., Auken, E., and Viezzoli, A., 2011, Quantification of modeling errors in airborne TEM caused by inaccurate system description. *Geophysics*, **76**, F43–F52. doi:10.1190/1.3511354
- Fitzpatrick, A., and Munday, T. J., 2005, Forward modelling airborne electromagnetic data for application in mapping the Coffin Bay groundwater lens: *CRCLEME restricted report*.
- Foged, N., Christiansen, A. V., and Auken, E., 2010, Validating SkyTEM data against ground-based TEM data at the Danish national test site by upward continuation: *Extended Abstract B27, Near Surface 2010, 16th European Meeting of Environmental and Engineering Geophysics, 6–8 September 2010, Zurich, Switzerland*.
- Green, A., and Lane, R., 2003, Estimating noise levels in AEM data: *Extended abstracts of the ASEG meeting, Adelaide 2003*.
- Green, A. A., and Munday, T., 2004, Forward modelling airborne electromagnetic data for the Riverland, S.A.: CRC LEME Open File Report 171, 1–36.
- Gunning, J., Glinzky, M. E., and Hedditch, J., 2010, Resolution and uncertainty in 1D CSEM inversion: a Bayesian approach and open-source implementation. *Geophysics*, **75**, F151–F171.
- Imman, J. R. Jr., Ryu, J., and Ward, S. H., 1975, Resistivity inversion. *Geophysics*, **38**, 1088–1108.
- Lane, R., Green, A., Golding, C., Owers, M., Pik, P., Plunkett, C., Sattel, D., and Thorn, B., 2000, An example of 3D conductivity mapping using the TEMPEST airborne electromagnetic system. *Exploration Geophysics*, **31**, 162–172. doi:10.1071/EG00162
- Lawrie, K. C., Munday, T., Clarke, J. D. A., Fitzpatrick, A., Cullen, K., Apps, H. E., Brodie, R. S., Ransley, T., Cahill, K., Lane, R., Richardson, M., English, P., and Hatch, M., 2009, Broken Hill managed aquifer recharge project: *Report no. 2009/03, Geoscience Australia*.
- Malinverno, A., 2002, Parsimonious Bayesian Markov chain Monte Carlo inversion in a nonlinear geophysical problem. *Geophysical Journal International*, **151**, 675–688. doi:10.1046/j.1365-246X.2002.01847.x
- Menke, W., 1989, *Geophysical data analysis: Discrete inverse theory*: Academic Press Inc.
- Minsley, B., 2011, A trans-dimensional Bayesian Markov chain Monte Carlo algorithm for model assessment using frequency-domain electromagnetic data. *Geophysical Journal International*, **187**, 252–272. doi:10.1111/j.1365-246X.2011.05165.x

- Munday, T. J., Brodie, R., Green, A., Lane, R., Sattel, D., Cook, P., Barnett, S., and Walker, G., 2003, Developing recharge reduction strategies in the Riverland of South Australia using airborne electromagnetic data — a case study in tailoring airborne geophysics given a particular target and a desired set of outcomes: *Extended Abstracts of the ASEG 16th International Geophysical Conference and Exhibition, Adelaide, 16–19 February 2003*.
- Oldenburg, D. W., and Li, Y., 1999, Estimating depth of investigation in dc resistivity and IP surveys. *Geophysics*, **64**, 403–416. doi:10.1190/1.1444545
- Serban, D. Z., and Jacobsen, B. H., 2001, The use of broadband prior covariance for inverse palaeoclimate estimation. *Geophysical Journal International*, **147**, 29–40. doi:10.1046/j.0956-540x.2001.01509.x
- Sharma, S. P., and Kaikkonen, P., 1999, Appraisal of equivalence and suppression problems in 1D EM and DC measurements using global optimization and joint inversion. *Geophysical Prospecting*, **47**, 219–249. doi:10.1046/j.1365-2478.1999.00121.x
- Sørensen, K. I., and Auken, E., 2004, SkyTEM – A new high-resolution helicopter transient electromagnetic system. *Exploration Geophysics*, **35**, 191–199.
- Tølbøll, R. J., and Christensen, N. B., 2006, Robust 1D inversion and analysis of helicopter electromagnetic (HEM) data. *Geophysics*, **71**, G53–G62. doi:10.1190/1.2187752